Entanglement measures for non-conformal D-branes

Arindam Lala[*]

Instituto de Física,
Pontificia Universidad Católica de Valparaíso,
Casilla 4059, Valparaíso, Chile

Abstract

We study various entanglement measures associated with certain non-conformal field theories. We consider nonconformal Dp-brane backgrounds which are dual to these field theories for our holographic analysis. Restricting our interests in p = 1, 2, 4, we explicitly compute properties of holographic entanglement entropy (HEE) and entanglement wedge cross section (EWCS) corresponding to two parallel strip shaped boundary subregions in these set ups. We study low and high temperature behaviours of these quantities analytically as well as using numerical methods. In all cases the EWCS decrease monotonically with temperature. We observe that for p < 3 it jumps discontinuously to zero, whereas for p > 3 it decays to zero in a continuous manner. However, in all cases the holographic mutual information (HMI) continuously decreases to zero. We also notice that the conjectured inequality between EWCS and HMI still holds even for non-conformal field theories. We analytically determine the critical separation between these subregions that triggers a phase transition in the holographic mutual information.

1 Introduction

The Gauge/Gravity duality [1, 2, 3] has enriched our understanding of concepts related to quantum information theory. Perhaps the most prominent of all these examples is the holographic computations of entanglement entropy of the dual boundary theory of interest which is particularly useful in determining the entanglement entropy of pure states [4, 5, 6]. This holographic entanglement entropy (HEE) proposal presents an interpretation of the entanglement entropy of the boundary field theory in terms of a geometric quantity, namely the minimal surface which is extended into the bulk. However, this prescription can easily be extended to the case of more than one boundary intervals. In this regard, a related quantity known as the holographic mutual information (HMI), $\mathtt{I}_M(A, B)$, between two disjoint boundary intervals A and B can be determined [7, 8, 9]. Interestingly $\mathtt{I}_M(A, B) \geq 0$ and it is also UV finite. Moreover, it undergoes a phase transition at some critical separation between the two intervals in which case the two subsystems become disentangled [8].

On the other hand, in order to determine the entanglement entropy of mixed states an interesting measure known as the holographic entanglement wedge cross section (EWCS), $\mathtt{E}_W$, is of much discussion in recent times [10, 11]. It is defined to be proportional to the minimal area of the entanglement wedge constructed out of the two intervals A and B[1]. This quantity is conjectured to be

---

[*]arindam.physics1@gmail.com, arindam.lala@pucv.cl

[1]The entanglement wedge is a bulk region whose boundary is given by $\partial W_{AB} = A \cup B \cup \Gamma^m_{AB}$. Here Γ^m_{AB} is the minimal surface associated with the union AB.

holographic dual to entanglement of purification (EoP) [12] which measures the correlation between A and B and, for pure states, reduces to entanglement entropy. It must be stressed that, although this proposal still has not been fully understood, there are certain indirect tests that this conjecture has passed, such as the following inequality [12],

$$\mathrm{E}_W \geq \frac{\mathrm{I}_M(A, B)}{2},\tag{1}$$

which has been proven explicitly using the holographic duality [10, 11]. Very recently, based on the formalism developed in [10, 11], various properties of EWCS along with HEE and HMI have been studied in different holographic set-ups [13, 14, 15, 16, 17]. All these examples mostly deal with conformal boundary theories in which cases the inequality (1) holds explicitly. Moreover, both E_W and HMI decrease monotonically and E_W is shown to undergo a discontinuous phase transition at high temperature.[2]

The purpose of the present paper is to extend the study of certain aspects of EWCS and HEE in non-conformal field theories which are dual to non-conformal Dp-branes [18, 19, 20]. The holographic correspondence between non-conformal Dp-branes and their dual field theories were studied in details in [18] where the (super) gravity description is controlled by an effective dimensionless coupling constant g_{eff}. However, in a more general set up the 10-dimensional theory of [18] can be dimensionally reduced to obtain an effective $(p+2)$-dimensional theory described by Einstein-dilaton gravity [19, 20]. Interestingly the space-time metric obtained in the later case is found to be conformal to that of AdS_{p+2}.

In this paper we study the EWCS of two disjoint boundary intervals in the shape of parallel strips each of width ℓ and length L. The low as well as high temperature behaviours of the EWCS are also studied. We restrict ourselves to the cases $\mathrm{p} = 1, 2, 4$. We also discuss about the behaviours of the HEE corresponding to the thermal boundary field theory along the line of analysis of [9, 21, 22]. In our analysis we observe that, in the mixed thermal state the EWCS scales with the area of the entangling region contrary to the volume scaling of the HEE. In addition, it monotonically decreases to zero value for large temperatures beyond certain critical value of the separation h between the two disjoint intervals at which they become disentangled. While for D4-branes this decay is continuous, it drops down to to zero value discontinuously for the D1- and D2-branes. However in all cases the corresponding HMI are monotonically decreasing functions as the critical separation between the strips is approached. Moreover, we also check the validity of the above inequality (1) explicitly in these set-ups.

The paper is organized as follows. In Section 2 we give a brief account of the non-conformal gravity backgrounds. In Section 3 we provide the computation of the EWCS and HEE corresponding to the strip shaped regions. The low and high temperature behaviours of these quantities are studied subsequently. The values of the critical distance of separation between the entangling regions are also determined. We finally conclude in Section 4.

2   The holographic set up

In this paper we study quantum information quantities for certain non-conformal field theories. In order to do so, we consider nonconformal Dp-brane backgrounds dual to these field theories [18]. Here we first very briefly mention the corresponding constructions provided in [18] and then review

---

[2]Note that, in [14] non-monotonous behaviours of HMI and EWCS has been reported, however in a different holographic set-up.

a more general dimensionally reduced model following [19] which we subsequently consider in all our computations.

The background generated from N coincident extremal Dp-branes in the string frame can be written as [18]

$$ds^2 = \alpha' \left[\frac{U^{(7-p)/2}}{g_{YM}\sqrt{d_p N}} \left(-dt^2 + \sum_{i=1}^{p} dx_i^2 \right) + \frac{g_{YM}\sqrt{d_p N}}{U^{(7-p)/2}} dU^2 + g_{YM}\sqrt{d_p N} U^{(p-3)/2} d\Omega_{8-p}^2 \right],$$

$$e^\phi = (2\pi)^{2-p} g_{YM}^2 \left(\frac{g_{YM}^2 N d_p}{U^{7-p}} \right)^{\frac{3-p}{4}}, \tag{2}$$

where

$$d_p = 2^{7-p} \pi^{\frac{9-3p}{2}} \Gamma\left(\frac{7-p}{2} \right), \qquad U = \frac{r}{\alpha'}, \tag{3}$$

and the limits $g_{YM}^2 \sim g_s \alpha'^{\frac{p-3}{2}} = $ fixed, $U = $ fixed and $\alpha' \to 0$ have been taken. On top of that, the validity of the supergravity description is controlled by the dimensionless coupling constant $g_{eff} = g_{YM}^2 N U^{p-3}$. In the non-extremal limit the above solution (2) can be expressed as

$$ds^2 = \alpha' \left[\frac{U^{(7-p)/2}}{g_{YM}\sqrt{d_p N}} \left(-f(U)dt^2 + \sum_{i=1}^{p} dx_i^2 \right) + \frac{g(U)g_{YM}\sqrt{d_p N}}{U^{(7-p)/2}} dU^2 + g_{YM}\sqrt{d_p N} U^{(p-3)/2} d\Omega_{8-p}^2 \right],$$

$$e^\phi = (2\pi)^{2-p} g_{YM}^2 \left(\frac{g_{YM}^2 N d_p}{U^{7-p}} \right)^{\frac{3-p}{4}}, \tag{4}$$

where

$$f(U) = 1 - \frac{U_0^{7-p}}{U^{7-p}}, \qquad g(U) = \frac{1}{f(U)} \approx 1 + \frac{U_0^{7-p}}{U^{7-p}}. \tag{5}$$

However, in a more general set up, we can perform an S^{8-p} Kaluza-Klein compactification of the above string-frame metric (4) to $(p+2)$-dimensions. The effective theory (in the Einstein frame) is then characterized by the $(p+2)$-dimensional Einstein-Dilaton action [19, 20]

$$S = \frac{N^2}{16\pi G_n^{p+2}} \left[\int d^{p+2}x \sqrt{-g} \left(\mathcal{R} - \frac{1}{2}\partial_\mu \Phi \partial^\mu \Phi + V(\Phi) \right) - 2 \int d^{p+1}x \sqrt{-\gamma} \mathcal{K} \right], \tag{6}$$

where

$$V(\Phi) = \frac{1}{2}(9-p)(7-p)N^{-2\lambda/p}e^{a\Phi}, \qquad \Phi = \frac{2\sqrt{2(9-p)}}{\sqrt{p}(7-p)}\phi, \tag{7}$$

$$a = -\frac{\sqrt{2}(p-3)}{\sqrt{p(9-p)}}, \qquad \lambda = \frac{2(p-3)}{(7-p)}, \tag{8}$$

and $\mathcal{K}$, γ_{ab} are the extrinsic curvature and the induced boundary metric, respectively. Also in (6) G_n^{p+2} is the $(p+2)$-dimensional Newton's constant. The above theory (6) allows for black brane solutions given by [19, 20]

$$ds^2 = \left(N e^\phi \right)^{\frac{2\lambda}{p}} \left[\frac{u^2}{\Delta^2} \left(-f(u)dt^2 + \sum_{i=1}^{p} dx_i^2 \right) + \frac{\Delta^2 du^2}{u^2 f(u)} \right], \tag{9a}$$
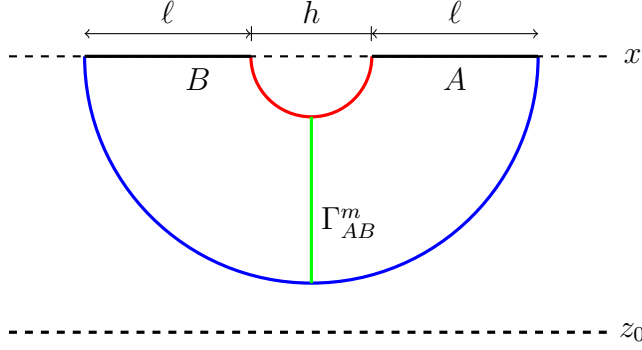
3

Figure 1: A schematic 2D diagram for computing entanglement wedge cross section (EWCS) Γ^m_{AB}. Here we consider two parallel strips each of width ℓ separated by h. Here z_0 represents the horizon of the brane.

$$f(u) = 1 - \left(\frac{u_0}{u}\right)^{\frac{2(7-p)}{(5-p)}}, \tag{9b}$$

$$e^\phi = \frac{1}{N}\left(g^2_{YM}N\right)^{\frac{7-p}{2(5-p)}}\left(\frac{u}{\Delta}\right)^{\frac{(p-7)(p-3)}{2(p-5)}}, \tag{9c}$$

$$u_0^2 = \frac{U_0^{5-p}}{(g^2_{YM}N)}, \qquad \Delta = \frac{2}{5-p}. \tag{9d}$$

Now the Hawking temperature of the Dp-brane can be computed by the usual method of analytical continuation of the metric (9a) to the Euclidean sector, $t \to i\tau$ [23]. The resulting expression for the temperature can be calculated as

$$T = \frac{1}{4\pi\Delta^2}\frac{2(p-7)}{(p-5)z_0}, \tag{10}$$

where the following change in coordinates $u \to 1/z$ and $u_0 \to 1/z_0$ has been taken into account [20].

On the other hand, the thermal entropy of the Dp-branes can be computed as

$$\begin{aligned}
S_{\text{th}} &= \frac{1}{4G_n^{p+2}}\int_{-\ell/2}^{\ell/2}\mathrm{d}x\int_{-L/2}^{L/2}\prod_{i=1}^{p-1}\mathrm{d}x_i\left(g_{xx}\prod_{i=1}^{p-1}g_{x_ix_i}\right)^{\frac{1}{2}}\\
&= \frac{L^{p-1}\ell}{4G_n^{p+2}}\left(g^2_{YM}N\right)^{\frac{p-3}{5-p}}\left(\frac{1}{z_0\Delta}\right)^{\frac{p-9}{p-5}}.
\end{aligned} \tag{11}$$

3   Entanglement Wedge Cross Section (EWCS)

Let us consider two long parallel strips each of width ℓ and separated by a distance h. They indeed represent two subregions A and B and is shown as dark black lines in Fig.1. We choose the following specific symmetric (around $x = 0$) configurations for the subsystems [13, 14, 15]:

$$A = \left\{\frac{h}{2} < x < \ell + \frac{h}{2}; \qquad -\frac{L}{2} < x_2, x_3, \cdots, x_{p-1} < \frac{L}{2}\right\}, \tag{12a}$$

$$B = \left\{-\ell - \frac{h}{2} < x < -\frac{h}{2}; \qquad -\frac{L}{2} < x_2, x_3 \cdots, x_{p-1} < \frac{L}{2}\right\}. \tag{12b}$$

4

Now the minimal surface, Γ^m_{AB}, that separates the two subsystems A and B is given by the vertical constant x surface at $x = 0$ which is a space-like slice. The induced metric on this slice can be written as

$$ds^2_{\Gamma^m_{AB}} = \left(Ne^\phi\right)^{\frac{2\lambda}{p}} \left[\frac{1}{z^2\Delta^2} \sum_{i=1}^{p-1} dx_i^2 + \frac{\Delta^2 dz^2}{z^2 f(z)} \right],$$

$$f(z) = 1 - \left(\frac{z}{z_0}\right)^{\frac{2(7-p)}{(5-p)}}. \tag{13}$$

Next we use the general expression for the entanglement wedge cross section (EWCS) corresponding to the two subregions A and B given by [10, 11, 13, 14, 15]

$$E_W = \frac{\text{Area}(\Gamma^m_{AB})}{4G_n^{p+2}}. \tag{14}$$

Using (13) and (14) we finally obtain[3]

$$E_W = \frac{L^{p-1}(g^2_{YM}N)^{\frac{p-3}{5-p}}}{4G_n^{p+2}\Delta^{\frac{p-1}{5-p}}} \int_{z_t(h)}^{z_t(2\ell+h)} dz\, \frac{z^{\frac{9-p}{p-5}}}{\sqrt{f(z)}}$$

$$= \frac{L^{p-1}(g^2_{YM}N)^{\frac{p-3}{5-p}}}{4G_n^{p+2}\Delta^{\frac{p-1}{5-p}}} \sum_{n=0}^{\infty} \frac{\Gamma\left(n+\frac{1}{2}\right)(p-5)}{\sqrt{\pi}(4+2n(p-7))\Gamma(n+1)} \left(\frac{z_t(2\ell+h)^\delta}{z_0^{n\alpha}} - \frac{z_t(h)^\delta}{z_0^{n\alpha}} \right), \tag{15}$$

where we have denoted

$$\alpha = \frac{2(7-p)}{(5-p)}, \qquad \delta = \frac{4+2n(p-7)}{(p-5)}. \tag{16}$$

We now use the Ryu-Tagayanagi prescription [4, 5] in order to find the holographic entanglement entropy (HEE) corresponding to a strip shaped region in the boundary of the geometry (9a). We choose the strip parametrized as

$$-\frac{\ell}{2} \le x \le \frac{\ell}{2}, \qquad -\frac{L}{2} \le x_2, \cdots, x_{p-1} \le \frac{L}{2}. \tag{17}$$

Thus the HEE functional can be wriiten as

$$S_{\text{EE}} = \frac{L^{p-1}}{4G_n^{p+2}} (g^2_{YM}N)^{\frac{p-3}{5-p}} \Delta^{\frac{9-p}{p-5}} \int dz\, z^{\frac{9-p}{p-5}} \sqrt{x'^2 + \frac{\Delta^4}{f(z)}}. \tag{18}$$

Interestingly, the above functional (18) has no explicit dependence on $x(z)$, and hence we can find the following first integral of motion by applying the conservation of energy of the system,

$$x'(z) = \pm \frac{\Delta^2}{\sqrt{f(z)\left(\left(\frac{z}{z_t}\right)^{2\frac{(9-p)}{(p-5)}} - 1\right)}}, \tag{19}$$

where z_t is the *turning point* of the minimal surface. Also note that, in deriving (19) we have used the boundary condition $\lim_{x\to\infty} z = z_t$.

---

[3]Notice that the integration in (15) can be evaluated exactly; however, it is convenient to express it in the series form [9, 21].
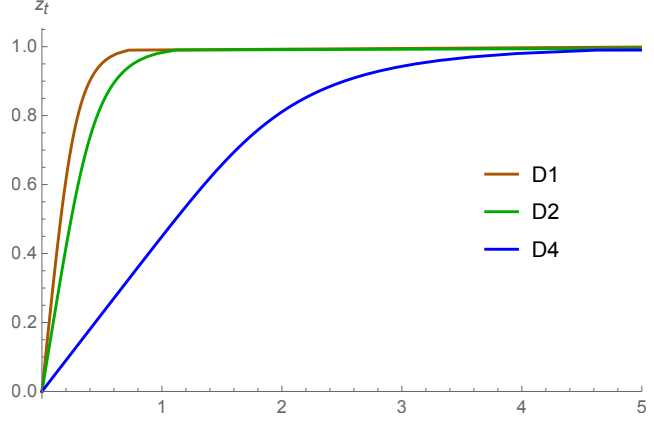
Figure 2: z_t *vs.* ℓ plot for different Dp-brane backgrounds. Here we set $z_0 = 1$.

In the next step we integrate (19) to obtain a relation between strip width ℓ and the turning point z_t as

$$\ell = 2\Delta^2 z_t \int_0^1 dv \frac{v^{\frac{9-p}{5-p}}}{\sqrt{f(v)}\sqrt{1 - v^{2\frac{(9-p)}{(5-p)}}}},\tag{20}$$

where we have defined $v = \frac{z}{z_t}$ and considered the fact that $1 \le p \le 4$.

Substituting (19) into (18) we finally obtain

$$S_{\text{EE}} = \frac{L^{p-1}}{4G_n^{p+2}}\left(g_{YM}^2 N\right)^{\frac{p-3}{5-p}} \frac{\Delta^{\frac{p-1}{p-5}}}{z_t^{\frac{4}{5-p}}} \int_0^1 \frac{dv}{v^{\frac{9-p}{5-p}}} \frac{1}{\sqrt{f(v)\left(1 - v^{2\frac{(9-p)}{(5-p)}}\right)}}.\tag{21}$$

The integrations appearing in the above equations (20) and (21) can be evaluated easily; and hence the width and the HEE can respectively be expressed as [9, 21]

$$\ell = \Delta^2 z_t \sum_{n=0}^{\infty} \frac{\Gamma\left(n + \frac{1}{2}\right)\Gamma\left(\frac{(n+1)(p-7)}{p-9}\right)}{\Gamma(n+1)\Gamma\left(\frac{3}{2} + n + \frac{2(n+1)}{(p-9)}\right)} \frac{(p-5)}{(p-9)}\left(\frac{z_t}{z_0}\right)^{2n\frac{(7-p)}{(5-p)}},\tag{22}$$

$$S_{\text{EE}} = S_{\sin} + \frac{L^{p-1}}{4G_n^{p+2}}\left(g_{YM}^2 N\right)^{\frac{p-3}{5-p}} \frac{\Delta^{\frac{p-1}{p-5}}}{z_t^{\frac{4}{5-p}}}\left[\frac{\sqrt{\pi}(p-5)\Gamma\left(\frac{2}{p-9}\right)}{2(p-9)\Gamma\left(\frac{p-5}{2(p-9)}\right)}\right.$$
$$\left.+\sum_{n=1}^{\infty} \frac{\Gamma\left(n + \frac{1}{2}\right)\Gamma\left(n + \frac{2(n+1)}{p-9}\right)}{\Gamma(n+1)\Gamma\left(\frac{p-5+2n(p-7)}{2(p-9)}\right)} \frac{(p-5)}{2(p-9)}\left(\frac{z_t}{z_0}\right)^{2n\frac{(7-p)}{(5-p)}}\right],\tag{23}$$

where the singular part of the HEE can be written as

$$S_{\sin} = \frac{L^{p-1}}{4G_n^{p+2}}\left(g_{YM}^2 N\right)^{\frac{p-3}{5-p}} \frac{\Delta^{\frac{p-1}{p-5}}}{\epsilon^{\frac{4}{5-p}}}\left(\frac{5-p}{4}\right).\tag{24}$$

Notice that in (24) ϵ is the ultraviolet (UV) cut-off.

6

3.1 Low and high temperature behaviours of the HEE

In this section we study both the low and high temperature behaviours of the holographic entanglement entropy (HEE) (23) in the backgrounds (9a). In order to achieve this analytically we need solve the turning point z_t in terms of the subregion length ℓ. It is evident from (22) that this procedure can only be applied in the low and high temperature limits.

The low temperature limit is geometrically realized when the turning point z_t corresponding to the RT surface(s) lies far away from the horizon z_0 of the black brane in the deep interior of the bulk: $z_t \ll z_0$. On the other hand, for the considered range of values of p, $1 \leq p \leq 4$, the exponent $\frac{(7-p)}{(5-p)} \leq 3$. Hence it is sufficient to keep terms upto order $\mathcal{O}\left(4\frac{(7-p)}{(5-p)}\right)$ in the perturbative expansion. Thus the resulting expression for the turning point in (22) may be written as

$$
z_t \approx \frac{\ell}{\Delta^2 \Upsilon}\left[1 - \frac{\sqrt{\pi}(p-5)\Gamma\left(\frac{2(p-7)}{p-9}\right)}{2(p-9)\Gamma\left(\frac{5}{2}+\frac{4}{p-9}\right)}\frac{1}{\Upsilon}\left(\frac{\ell}{\Delta^2 z_0 \Upsilon}\right)^{\frac{2(7-p)}{(5-p)}} + \left\{\left(\frac{\sqrt{\pi}(p-5)\Gamma\left(\frac{2(p-7)}{p-9}\right)}{2(p-9)\Gamma\left(\frac{5}{2}+\frac{4}{p-9}\right)}\frac{1}{\Upsilon}\right)^2\right.\right.
$$
$$
\left.\left. - \left(\frac{3\sqrt{\pi}(p-5)}{8(p-9)}\frac{\Gamma\left(\frac{3(p-7)}{(p-9)}\right)}{\Gamma\left(\frac{7}{2}+\frac{6}{p-9}\right)}\frac{1}{\Upsilon}\right)\right\}\left(\frac{\ell}{\Delta^2 z_0 \Upsilon}\right)^{\frac{4(7-p)}{(5-p)}} + \mathcal{O}\left(\frac{\ell}{\Delta^2 z_0 \Upsilon}\right)^{\frac{6(7-p)}{(5-p)}}\right],
\tag{25}
$$

where we have defined

$$
\Upsilon = \frac{\sqrt{\pi}(p-5)\,\Gamma\left(\frac{p-7}{p-9}\right)}{(p-9)\,\Gamma\left(\frac{3}{2}+\frac{2}{p-9}\right)}.
\tag{26}
$$

With this approximation and substituting (25) into (23) the final expressions for the HEE at low temperatures can be written as follows.[4]

D1-brane

$$
S_{\mathrm{EE}_{LT}}^{(D1)} = \bar{\mathsf{C}}_1\left[S_0 + \mathcal{C}_1\left(\frac{1}{\ell}\right)\left(1 + \mathcal{C}_2\left(\frac{\pi T\ell}{3}\right)^3 + \mathcal{C}_3\left(\frac{\pi T\ell}{3}\right)^6 + \mathcal{O}(\pi T\ell/3)^7\right)\right],
\tag{27}
$$

where we have denoted

$$
\bar{\mathsf{C}}_1 = \frac{(g_{YM}^2 N)^{-\frac{1}{2}}}{4G_n^3}, \qquad\qquad S_0 = \frac{1}{\epsilon},
\tag{28}
$$

and the other *constants* $\mathcal{C}_1$, $\mathcal{C}_2$ and $\mathcal{C}_3$ are combinations of the gamma functions which we omit writing here.

D2-brane

$$
S_{\mathrm{EE}_{LT}}^{(D2)} = \bar{\mathsf{C}}_2\left[S_0 + \mathcal{D}_1\left(\frac{1}{\ell}\right)^{4/3}\left(1 + \mathcal{D}_2\left(\frac{8\pi T\ell}{15}\right)^{10/3} + \mathcal{D}_3\left(\frac{8\pi T\ell}{15}\right)^{20/3} + \mathcal{O}(8\pi T\ell/15)^{19/3}\right)\right],
\tag{29}
$$

---

[4]Here and what follows, the subscripts 'LT' and 'HT' denote Low Temperature and High Temperature, respectively.

where

$$\bar{\mathsf{C}}_2 = \frac{L(g_{YM}^2 N)^{-\frac{1}{3}}}{4G_n^4 \Delta^{\frac{1}{3}}}, \qquad\qquad S_0 = \left(\frac{3}{4}\right)\left(\frac{1}{\epsilon}\right)^{4/3}, \qquad (30)$$

and $\mathcal{D}_1$, $\mathcal{D}_2$ and $\mathcal{D}_3$ are constants.

D4-brane

$$S_{\mathrm{EE}_{LT}}^{(D4)} = \bar{\mathsf{C}}_4 \left[S_0 + \mathcal{E}_1 \left(\frac{1}{\ell}\right)^4 \left(1 + \mathcal{E}_2 \left(\frac{8\pi T\ell}{3}\right)^6 + \mathcal{E}_3 \left(\frac{8\pi T\ell}{3}\right)^{12} + \mathcal{O}(8\pi T\ell/3)^{18} \right) \right], \qquad (31)$$

with

$$\bar{\mathsf{C}}_4 = \frac{L^3 (g_{YM}^2 N)}{4G_n^6 \Delta^3}, \qquad\qquad S_0 = \left(\frac{1}{4}\right)\left(\frac{1}{\epsilon}\right)^4, \qquad (32)$$

and $\mathcal{E}_1$, $\mathcal{E}_2$ and $\mathcal{E}_3$ are constants.

On the other hand, at high temperatures the turning point z_t approaches the horizon of the black branes, $z_t \to z_0$, and indeed wraps a part of the horizon. Thus the leading contribution comes from the near horizon part of the surface. On top of that, the entire bulk geometry contributes in the form of subleading terms [9, 21]. The following combination is found to be converging as the limit $z_t \to z_0$ is taken and hence we proceed our analysis with this combination [9, 15, 21].

$$S_{\mathrm{EE}} - \frac{L^{p-1}(g_{YM}^2 N)^{\frac{p-3}{5-p}}}{4G_n^{p+2}} \left(\frac{1}{\Delta z_t}\right)^{\frac{9-p}{5-p}} \ell = \frac{L^{p-1}(g_{YM}^2 N)^{\frac{p-3}{5-p}}}{4G_n^{p+2} \Delta^{\frac{p-1}{5-p}}} \left(\frac{1}{z_t}\right)^{\frac{4}{5-p}} \int_{\epsilon/z_t}^1 dv \frac{\sqrt{1 - v^{\frac{2(9-p)}{5-p}}}}{\sqrt{f(v)}\, v^{\frac{9-p}{5-p}}}. \qquad (33)$$

Using (33) we can now recast the finite part of the HEE as

$$S_{\mathrm{EE}} = \frac{L^{p-1}(g_{YM}^2 N)^{\frac{p-3}{5-p}}}{4G_n^{p+2}} \left(\frac{1}{\Delta z_t}\right)^{\frac{9-p}{5-p}} \ell + \frac{L^{p-1}(g_{YM}^2 N)^{\frac{p-3}{5-p}}}{4G_n^{p+2} \Delta^{\frac{p-1}{5-p}}} \left(\frac{1}{z_t}\right)^{\frac{4}{5-p}} \left[\frac{(p-5)}{4} {}_2F_1\left(\frac{1}{2}, \frac{2}{p-9}; \frac{p-7}{p-9}; 1\right) \right.$$
$$\left. + \int_0^1 dv \left(\frac{\sqrt{1 - v^{\frac{2(9-p)}{5-p}}}}{\sqrt{f(v)}\, v^{\frac{9-p}{5-p}}} - \frac{1}{v^{\frac{9-p}{5-p}} \sqrt{1 - v^{\frac{2(9-p)}{5-p}}}} \right) \right], \qquad (34)$$

where ${}_2F_1(a, b; c; z)$ is the usual hypergeometric function.

Finally, considering the limit $z_t \to z_0$, we can read off the expression for the HEE at high temperatures from (34) as [9, 21]

$$S_{\mathrm{EE}_{HT}} = S_{\sin} + \frac{V(g_{YM}^2 N)^{\frac{p-3}{5-p}}}{4G_n^{p+2} \Delta^{\frac{9-p}{5-p}}} \left(\frac{2\pi \Delta^2 (p-5)}{(p-7)} T \right)^{\frac{9-p}{5-p}} \left\{ 1 + \left(\frac{(p-7)}{2\pi \ell T (p-5)} \right) \Theta \right\}, \qquad (35)$$

where $S_{\sin}$ is the singular part of the HEE given by (24) and

$$\Theta = \frac{\sqrt{\pi}(p-5)}{(p-9)} \left[\frac{\Gamma\left(\frac{2}{p-9}\right)}{2\Gamma\left(\frac{p-5}{2(p-9)}\right)} - \frac{\Gamma\left(\frac{p-7}{p-9}\right)}{\Gamma\left(\frac{3}{2} + \frac{2}{(p-9)}\right)} \right]$$
$$+ \sum_{n=1}^{\infty} \frac{(p-5)\Gamma\left(n + \frac{1}{2}\right)}{(p-9)\Gamma(n+1)} \left[\frac{\Gamma\left(n + \frac{2(n+1)}{p-9}\right)}{2\Gamma\left(\frac{p-5+2n(p-7)}{2(p-9)}\right)} - \frac{\Gamma\left(\frac{(n+1)(p-7)}{p-9}\right)}{\Gamma\left(\frac{3}{2} + n + \frac{2(n+1)}{(p-9)}\right)} \right]. \qquad (36)$$

Note that in (35) the volume of the strip is given by $V = \ell L^{p-1}$. Also the finite term in (35) is proportional to the thermal entropy (11). This is expected since at high temperature regime the contributions to the HEE of the thermal boundary field theory comes from the thermal fluctuations. Furthermore, the finite term of the HEE in (35) scales as the volume of the entangling region.

3.2 Low and high temperature behaviours of the EWCS

In order to study the low and high temperature behaviours of the EWCS we first notice that we can achieve this by taking into account the following three intrinsic scales associated with the theory: the separation distance h between the two entangling regions, the width ℓ of each of the regions and the temperature T of the boundary theory [9, 13, 14, 15, 21]. Subsequently, in this case the low temperature limit corresponds to $hT \ll \ell T \ll 1$. Note that this corresponds to considering the temperature smaller than both the length scales associated with h and ℓ. On the other hand, the high temperature limit may be defined by considering the following inequality $hT \ll 1 \ll \ell T$ in which case the temperature is large compared to the scale associated with ℓ but small compared to that associated with h.[5] Interestingly, this high temperature limit further amounts to taking the following two approximations: $z_t(h) \ll z_0$ and $z_t(2\ell + h) \to z_0$. The first approximation amounts to considering only the leading order term in the second term within the braces in (15), while in order the second approximation to be valid we must ensure the convergence of the first sum in (15). It is trivial to check that this is indeed the case. Thus it is safe to consider the limit $z_t(2\ell + h) \to z_0$.

Let us now discuss the different cases corresponding to $p = 1, 2, 4$ separately which correspond to D1-, D2- and D4-branes, respectively.

D1-branes

In the low temperature limit $hT \ll \ell T \ll 1$ the EWCS (15) for the D1-branes can be computed as

$$
\begin{aligned}
E_{W_{LT}}^{(D1)} &= \frac{(g_{YM}^2 N)^{-\frac{1}{2}}}{4G_n^3} \sum_{n=0}^{\infty} \frac{\Gamma(n + \frac{1}{2})}{\sqrt{\pi}\Gamma(n+1)} \left(\frac{z_t(2\ell + h)^{3n-1} - z_t(h)^{3n-1}}{3n-1} \right) \cdot \frac{1}{z_0^{3n}} \\
&= \frac{(g_{YM}^2 N)^{-\frac{1}{2}}}{4G_n^3} \left[\frac{\sqrt{\pi}\Gamma(\frac{3}{4})}{8\Gamma(\frac{5}{4})} \left(\frac{1}{h} - \frac{1}{2\ell + h} \right) + \frac{64\,\Gamma(\frac{5}{4})^2}{\pi\Gamma(\frac{3}{4})^2} \left(1 - \frac{\sqrt{\pi}\Gamma(\frac{5}{4})}{\Gamma(\frac{3}{4})} \right) \ell(\ell + h) \left(\frac{\pi T}{3} \right)^3 + \cdots \right],
\end{aligned}
$$
(37)

where we have used (10) and (25).

On the other hand, considering the aforementioned high temperature limits the behaviour of the EWCS can be determines as

$$
E_{W_{HT}}^{(D1)} \approx \frac{(g_{YM}^2 N)^{-\frac{1}{2}}}{4G_n^3} T \left[\frac{\pi\tilde{\mathcal{C}}_1}{3} + \frac{\sqrt{\pi}\Gamma(\frac{3}{4})}{8\Gamma(\frac{5}{4})} \left(\frac{1}{hT} \right) + \frac{16\pi^{\frac{5}{2}}}{27} \left(\frac{\Gamma(\frac{5}{4})}{\Gamma(\frac{3}{4})} \right)^3 (hT)^2 \right],
$$
(38)

where we have defined $\tilde{\mathcal{C}}_1 = \sum_{n=0}^{\infty} \frac{\Gamma(n + \frac{1}{2})}{\sqrt{\pi}(3n-1)\Gamma(n+1)}$.

D2-branes

---

[5]In our calculations we shall *not* take into account another limit $\ell T \ll hT$ or $1 \ll \ell T$, $1 \ll hT$ as this corresponds to the disentangling phase of the two subregions [9, 13, 15, 21, 22].

In a similar manner, the low temperature behaviour of EWCS for the D2-branes (15) can be determined as

$$
\begin{aligned}
\mathrm{E}_{W_{LT}}^{(D2)} &= \frac{L(g_{YM}^2 N)^{-\frac{1}{3}}}{4G_n^4 \Delta^{\frac{1}{3}}} \sum_{n=0}^{\infty} \frac{\Gamma\left(n+\frac{1}{2}\right)}{\sqrt{\pi}\Gamma(n+1)} \left(\frac{z_t(2\ell+h)^{\frac{10n-4}{3}} - z_t(h)^{\frac{10n-4}{3}}}{10n-4} \right) \cdot \frac{3}{z_0^{\frac{10}{3}n}} \\
&= \frac{L(g_{YM}^2 N)^{-\frac{1}{3}}}{4G_n^4 \Delta^{\frac{1}{3}}} \left[\frac{3(2\pi)^{\frac{2}{3}}}{(21)^{\frac{4}{3}}} \left(\frac{\Gamma\left(\frac{5}{7}\right)}{\Gamma\left(\frac{17}{14}\right)} \right)^{\frac{4}{3}} \left(\frac{1}{h^{\frac{4}{3}}} - \frac{1}{(2\ell+h)^{\frac{4}{3}}} \right) \right. \\
&\quad \left. + \frac{441}{16\pi} \frac{\Gamma\left(\frac{17}{14}\right)^2}{\Gamma\left(\frac{5}{7}\right)^2} \ell(\ell+h) \left(1 - \frac{2\Gamma\left(\frac{17}{14}\right)\Gamma\left(\frac{10}{7}\right)}{\Gamma\left(\frac{5}{7}\right)\Gamma\left(\frac{27}{14}\right)} \right) \left(\frac{8\pi T}{15} \right)^{\frac{10}{3}} + \cdots \right].
\end{aligned}
\tag{39}
$$

On the other hand, at high temperature the corresponding EWCS behaves as

$$
\begin{aligned}
\mathrm{E}_{W_{HT}}^{(D2)} &\approx \frac{L(g_{YM}^2 N)^{-\frac{1}{3}}}{4G_n^4 \Delta^{\frac{1}{3}}} T^{\frac{4}{3}} \left[\tilde{\mathcal{C}}_2 \left(\frac{8\pi}{15} \right)^{\frac{4}{3}} + \frac{3(2\pi)^{\frac{2}{3}}}{21^{\frac{4}{3}}} \left(\frac{\Gamma\left(\frac{5}{7}\right)}{\Gamma\left(\frac{17}{14}\right)} \right)^{\frac{4}{3}} \left(\frac{1}{hT} \right)^{\frac{4}{3}} \right. \\
&\quad \left. + \frac{441}{32\pi} \frac{\Gamma\left(\frac{17}{14}\right)^3 \Gamma\left(\frac{10}{7}\right)}{\Gamma\left(\frac{5}{7}\right)^3 \Gamma\left(\frac{27}{14}\right)} \left(\frac{8\pi}{15} \right)^{\frac{10}{3}} (hT)^2 \right],
\end{aligned}
\tag{40}
$$

with $\tilde{\mathcal{C}}_2 = \sum_{n=0}^{\infty} \dfrac{3\Gamma\left(n+\frac{1}{2}\right)}{\sqrt{\pi}(10n-4)\Gamma(n+1)}$.

D4-branes

Similar to previous two cases, the low temperature behaviour of EWCS (15) corresponding to the D4-brane is given by

$$
\begin{aligned}
\mathrm{E}_{W_{LT}}^{(D4)} &= \frac{2L^3(g_{YM}^2 N)}{G_n^6} \sum_{n=0}^{\infty} \frac{\Gamma\left(n+\frac{1}{2}\right)}{\sqrt{\pi}\Gamma(n+1)} \left(\frac{z_t(2\ell+h)^{6n-4} - z_t(h)^{6n-4}}{6n-4} \right) \cdot \frac{1}{z_0^{6n}} \\
&= \frac{2L^3(g_{YM}^2 N)}{G_n^6} \left[\frac{1028\pi^2 \Gamma\left(\frac{3}{5}\right)^4}{\Gamma\left(\frac{1}{10}\right)^4} \left(\frac{1}{h^4} - \frac{1}{(2\ell+h)^4} \right) \right. \\
&\quad \left. + \frac{25}{16\pi} \frac{\Gamma\left(\frac{11}{10}\right)^2}{\Gamma\left(\frac{3}{5}\right)^2} \left(1 - \frac{2\Gamma\left(\frac{11}{10}\right)\Gamma\left(\frac{6}{5}\right)}{\Gamma\left(\frac{3}{5}\right)\Gamma\left(\frac{17}{10}\right)} \right) \ell(\ell+h) \left(\frac{8\pi T}{3} \right)^6 + \cdots \right].
\end{aligned}
\tag{41}
$$

Also, at high temperature the corresponding EWCS behaves as

$$
\mathrm{E}_{W_{HT}}^{(D4)} \approx \frac{L^3(g_{YM}^2 N)}{4G_n^6 \Delta^3} T^4 \left[\tilde{\mathcal{C}}_4 \left(\frac{8\pi}{3} \right)^4 + \frac{1024\pi^2 \Gamma\left(\frac{3}{5}\right)^4}{\Gamma\left(\frac{1}{10}\right)^4} \left(\frac{1}{hT} \right)^4 + \frac{25}{32\pi} \frac{\Gamma\left(\frac{11}{10}\right)^3 \Gamma\left(\frac{6}{5}\right)}{\Gamma\left(\frac{3}{5}\right)^3 \Gamma\left(\frac{17}{10}\right)} \left(\frac{8\pi}{3} \right)^6 (hT)^2 \right],
\tag{42}
$$

where $\tilde{\mathcal{C}}_4 = \sum_{n=0}^{\infty} \dfrac{\Gamma\left(n+\frac{1}{2}\right)}{\sqrt{\pi}(6n-4)\Gamma(n+1)}$.

Let us now discuss the following observations that we can make from the low as well as high temperature behaviours of the EWCS derived above. These are listed as follows.
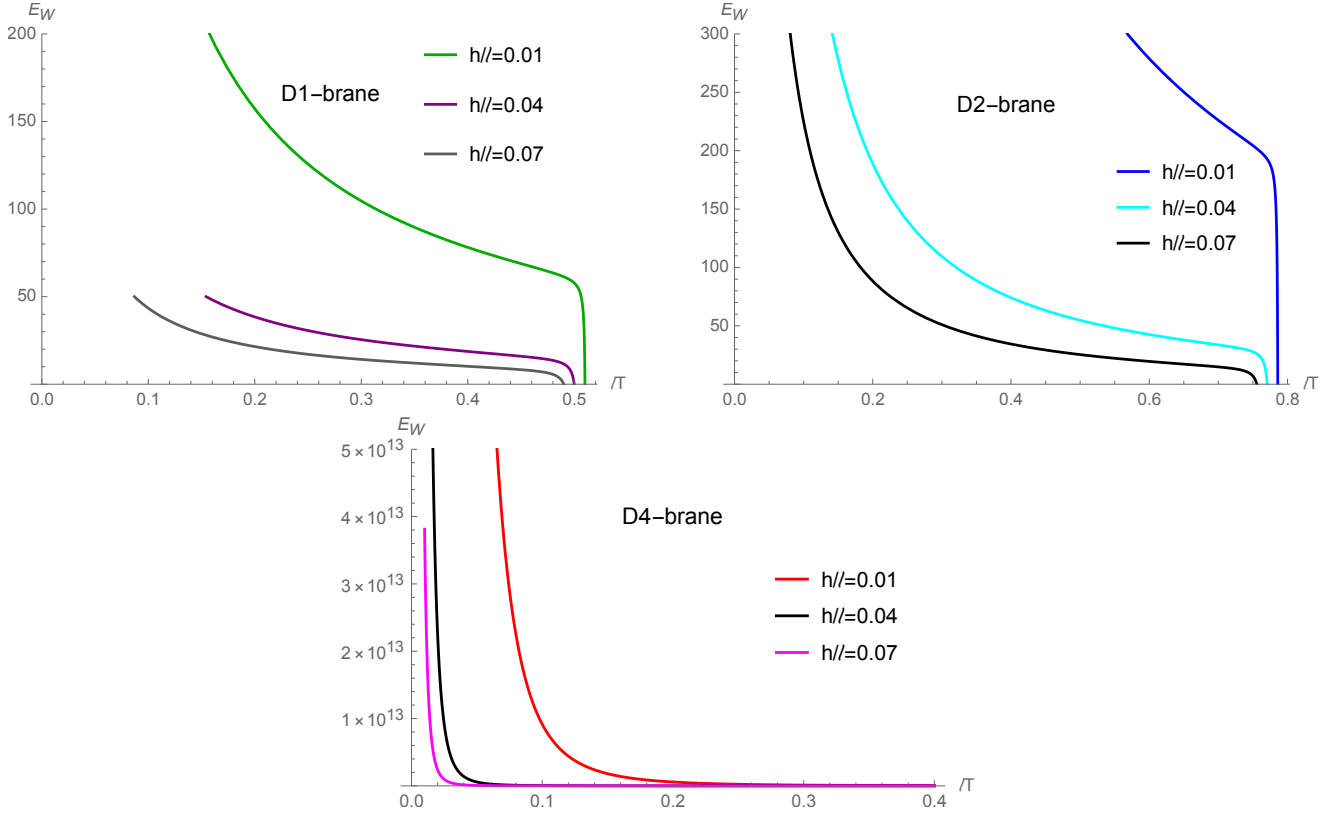
Figure 3: E_W *vs.* ℓT plots for different values of the dimensionless quantity h/ℓ. Clearly, as the temperatures ($\ell = 1$) increase E_W shows a decreasing behaviour.

- When the widths of the subsystems (ℓ) are small EWCS increase sharply, and beyond certain values of the width it drops down to zero value indicating a phase transition due to the disentanglement of the subsystems. For the intermediate values of ℓ the decrease in EWCS is monotonic.

- At low temperatures the first terms of the EWCS in (37), (39), (41) increase as the separation h between the two entangling regions decrease. Moreover, as $h \to 0$ the EWCS diverge. This is clearly visible from Fig.4. Also if we keep the width and separation between the two subregions fixed and increase the temperature, the EWCS decreases monotonically to zero ($E_W = 0$) in all cases indicating a phase transition resulting due to the disentanglement of the Ryu-Takayanagi surfaces. Notably, when p = 1, 2 this fall-off is discontinuous similar to the AdS cases. However, when p = 4 the EWCS becomes zero in a continuous manner (the bottom figure of Fig.4.). Clearly this later case is different from most of the cases that have been studied so far in the literature as far as our knowledge is concerned [13, 14, 15][6]. This is the most important observation that we make in this paper.

- The first terms in (38), (40), (42) is proportional to the area of the entangling region, L^{p-1}. This suggests that at finite temperature the EWCS obeys an area law. This is in sharp contrast to the HEE at high temperature obtained in (35) where it scales with the volume. Similar observations have in fact been made earlier [13, 14, 15]. Moreover, this are law scaling implies

---

[6]However, in [14] it was observed that breaking of conformal invariance in the background may result non-monotonous behaviours of HMI as well as EWCS.
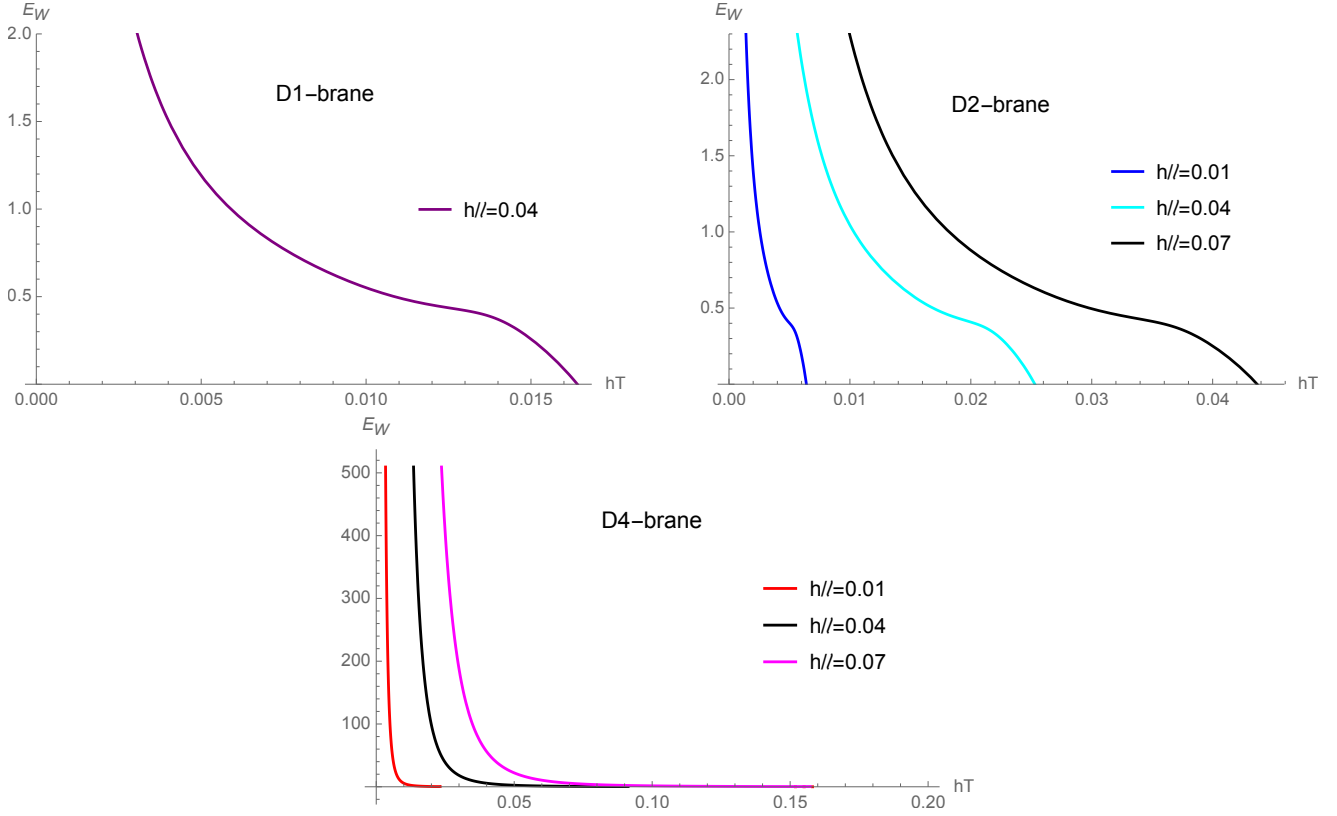
Figure 4: E_W *vs.* hT plots for different values of the dimensionless quantity h/ℓ.

that the EWCS carries more information than the HEE regarding the correlation between A and B [7, 8, 9, 13, 14, 15].

3.3   Critical separation between the strips

In this section we determine the critical separation between the parallel strips A and B at which these two subregions become completely disentangled. This can indeed be found by calculating the holographic mutual information (HMI) between A and B [7, 8, 9]. The HMI between the two subregions A and B can be expressed as [7, 8, 9, 13, 14, 15]

$$\mathtt{I}_M(\ell, h) = 2S(\ell) - S(h) - S(2\ell + h). \tag{43}$$

It measures the total correlations between A and B.

At the critical value of the separation, h_c, at which the two subregions are no longer entangled, we have

$$\mathtt{I}_M(\ell, h_c) = 0. \tag{44}$$

This is reminiscent of a first order phase transition which occurs due to the competition between different configurations for calculating $S(2\ell + h)$: when the separation distance is small the connected configuration is preferred over the disconnected one. On the other hand, for large separation the disconnected configuration is preferred resulting the vanishing of the HMI [8, 13]. This type of phase transitions occur for large values of the subsystem size $\ell \to \infty$. Thus $S(\ell)$ and $S(2\ell + h)$ are represented by the IR (high temperature) expression for the HEE while $S(h)$ is represented by the UV (low temperature) expression for the HEE [10, 11, 13, 14, 15].
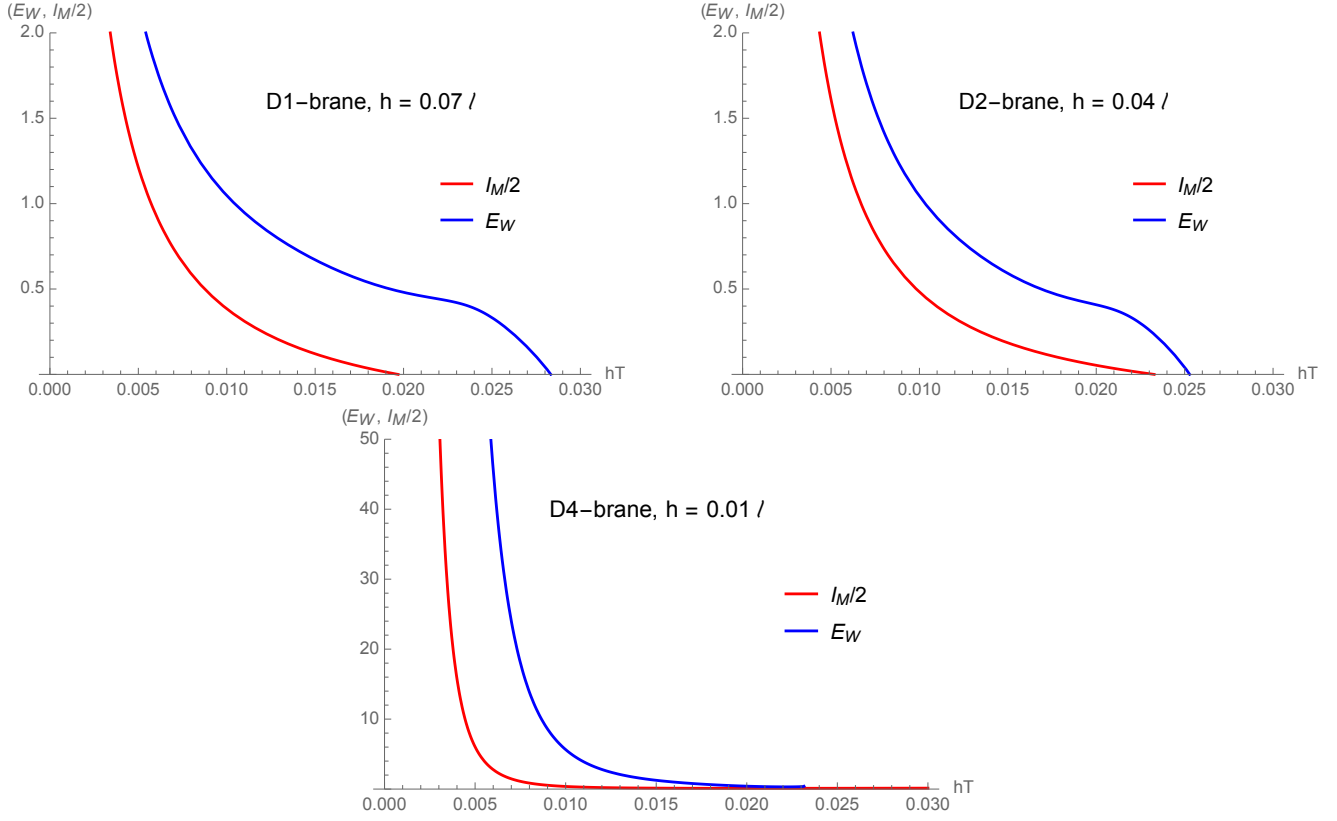
12

Figure 5: Holographic Mutual Information plots for different non-conformal backgrounds. Notice that in all three cases $E_W \geq I_M/2$.

Due to the complexity of the resulting expressions that arise from (44), below we only write down the general form of the equation for the critical separations (h_c) as

$$\sum_{i=0}^{4} a_i \left(\frac{h_c}{z_0} \right)^{n_i} = 0, \tag{45}$$

where we have used the results from Section 3.1. In (45) the numerical coefficients a_i are certain combinations of gamma functions whose explicit expressions we avoid writing here and the exponents n_i may be given as

for D1-brane $\quad (n_0 = 0, n_1 = 1, n_2 = 2, n_3 = 3, n_4 = 6),$

for D2-brane $\quad \left(n_0 = 0, n_1 = \frac{4}{3}, n_2 = \frac{7}{3}, n_3 = \frac{10}{3}, n_4 = \frac{20}{3} \right),$ (46)

for D4-brane $\quad (n_0 = 0, n_1 = 4, n_2 = 5, n_3 = 6, n_4 = 12).$

In the next step we explicitly check the inequality (1) by numerically plotting both E_W and $I_M(A, B)/2$ against the dimensionless quantity hT in Fig.5. In addition to validate (1), these plots also show the monotonically decreasing nature of both E_W and $I_M(A, B)$. Moreover, beyond the critical separation $h_c T$ ($T = 1$) determined by (45) both of them approach zero which is an essential nature for the phase transition discussed above [10, 11, 12].

4   Conclusions

In this paper we have studied aspects of holographic entanglement measures for certain class of non-conformal field theories which are holographic dual to non-conformal Dp-brane backgrounds [19, 20]. We explicitly computed entanglement wedge cross section (EWCS), holographic entanglement entropy (HEE) and the holographic mutual information (HMI) for these dual non-conformal field theories in the spirit of the Gauge/Gravity duality. In our analysis we considered $p = 1, 2, 4$ while $p = 3$ corresponds to the usual AdS_5/CFT_4 duality [1]. In our computations we considered a bipartite system with two parallel entangling regions of equal width ℓ and length L separated by a distance h. We observed different qualitative behaviours of the EWCS for $p < 3$ and $p > 3$. Although in all cases the EWCS shows a monotonically decreasing behaviour with the temperature, when $p < 3$ EWCS discontinuously drops down to zero value beyond a critical separation distance h_c between the entangling subregions. On the other hand, when $p = 4$ this decay to zero value is continuous. This is in sharp contrast to the usual conformal field theory set ups where for any values of the dimension the EWCS shows a discontinuous behaviour [13, 14, 15]. This later case is a reminiscent of the unconventional behaviour of EWCS in presence of non-conformality that was observed in [14], although in a different holographic set-up. However, in all cases the HMI decays to zero in continuous manner.

Finally, let us mention a few future directions that can be explored in the framework of the geometries that are considered in this paper. The continuous phase transition of the EWCS for $p = 4$ is still unclear to us. Naively it seems to be an effect of large N limit of the corresponding boundary theory similar to the case of HMI [24]. In this regard it will be interesting to find an appropriate justification to this behaviour. In this connection, it seems equally important to consider quantum corrections to both EWCS and HEE in these holographic set-ups [24].

Acknowledgments

References

[1] J. M. Maldacena, "The Large N limit of superconformal field theories and supergravity," Int. J. Theor. Phys. **38** (1999), 1113-1133, Adv. Theor. Math. Phys. 2 (1998) 231-252, doi:10.1023/A:1026654312961 [arXiv:hep-th/9711200 [hep-th]].

[2] E. Witten, "Anti-de Sitter space and holography," Adv. Theor. Math. Phys. **2** (1998), 253-291 doi:10.4310/ATMP.1998.v2.n2.a2 [arXiv:hep-th/9802150 [hep-th]].

[3] O. Aharony, S. S. Gubser, J. M. Maldacena, H. Ooguri and Y. Oz, "Large N field theories, string theory and gravity," Phys. Rept. **323** (2000), 183-386 doi:10.1016/S0370-1573(99)00083-6 [arXiv:hep-th/9905111 [hep-th]].

[4] S. Ryu and T. Takayanagi, "Holographic derivation of entanglement entropy from AdS/CFT," Phys. Rev. Lett. **96** (2006), 181602 doi:10.1103/PhysRevLett.96.181602 [arXiv:hep-th/0603001 [hep-th]].

[5] S. Ryu and T. Takayanagi, "Aspects of Holographic Entanglement Entropy," JHEP **08** (2006), 045 doi:10.1088/1126-6708/2006/08/045 [arXiv:hep-th/0605073 [hep-th]].

[6] V. E. Hubeny, M. Rangamani and T. Takayanagi, "A Covariant holographic entanglement entropy proposal," JHEP **07** (2007), 062 doi:10.1088/1126-6708/2007/07/062 [arXiv:0705.0016 [hep-th]].

[7] M. M. Wolf, F. Verstraete, M. B. Hastings and J. I. Cirac, "Area Laws in Quantum Systems: Mutual Information and Correlations," Phys. Rev. Lett. **100** (2008) no.7, 070502 doi:10.1103/PhysRevLett.100.070502 [arXiv:0704.3906 [quant-ph]].

[8] M. Headrick, "Entanglement Renyi entropies in holographic theories," Phys. Rev. D **82** (2010), 126010 doi:10.1103/PhysRevD.82.126010 [arXiv:1006.0047 [hep-th]].

[9] W. Fischler, A. Kundu and S. Kundu, "Holographic Mutual Information at Finite Temperature," Phys. Rev. D **87** (2013) no.12, 126012 doi:10.1103/PhysRevD.87.126012 [arXiv:1212.4764 [hep-th]].

[10] T. Takayanagi and K. Umemoto, "Entanglement of purification through holographic duality," Nature Phys. **14** (2018) no.6, 573-577 doi:10.1038/s41567-018-0075-2 [arXiv:1708.09393 [hep-th]].

[11] P. Nguyen, T. Devakul, M. G. Halbasch, M. P. Zaletel and B. Swingle, "Entanglement of purification: from spin chains to holography," JHEP **01** (2018), 098 doi:10.1007/JHEP01(2018)098 [arXiv:1709.07424 [hep-th]].

[12] B. M. Terhal, M. Horodecki, D. W. Leung and D. P. DiVincenzo, "The entanglement of purification," J. Math. Phys. **43** (2002) 4286 [quan-ph/0202044].

[13] K. Babaei Velni, M. R. Mohammadi Mozaffar and M. H. Vahidinia, "Some Aspects of Entanglement Wedge Cross-Section," JHEP **05** (2019), 200 doi:10.1007/JHEP05(2019)200 [arXiv:1903.08490 [hep-th]].

[14] N. Jokela and A. Pönni, "Notes on entanglement wedge cross sections," JHEP **07** (2019), 087 doi:10.1007/JHEP07(2019)087 [arXiv:1904.09582 [hep-th]].

[15] S. Chakrabortty, S. Pant and K. Sil, "Effect of back reaction on entanglement and subregion volume complexity in strongly coupled plasma," JHEP **06** (2020), 061 doi:10.1007/JHEP06(2020)061 [arXiv:2004.06991 [hep-th]].

[16] Y. f. Huang, Z. j. Shi, C. Niu, C. y. Zhang and P. Liu, "Mixed State Entanglement for Holographic Axion Model," Eur. Phys. J. C **80** (2020) no.5, 426 doi:10.1140/epjc/s10052-020-7921-y [arXiv:1911.10977 [hep-th]].

[17] G. Fu, P. Liu, H. Gong, X. M. Kuang and J. P. Wu, "Informational properties for Einstein-Maxwell-Dilaton Gravity," [arXiv:2007.06001 [hep-th]].

[18] N. Itzhaki, J. M. Maldacena, J. Sonnenschein and S. Yankielowicz, "Supergravity and the large N limit of theories with sixteen supercharges," Phys. Rev. D **58** (1998), 046004 doi:10.1103/PhysRevD.58.046004 [arXiv:hep-th/9802042 [hep-th]].

[19] H. J. Boonstra, K. Skenderis and P. K. Townsend, "The domain wall / QFT correspondence," JHEP **01** (1999), 003 doi:10.1088/1126-6708/1999/01/003 [arXiv:hep-th/9807137 [hep-th]].

[20] D. W. Pang, "Entanglement thermodynamics for nonconformal D-branes," Phys. Rev. D **88** (2013) no.12, 126001 doi:10.1103/PhysRevD.88.126001 [arXiv:1310.3676 [hep-th]].

[21] W. Fischler and S. Kundu, "Strongly Coupled Gauge Theories: High and Low Temperature Behavior of Non-local Observables," JHEP **05** (2013), 098 doi:10.1007/JHEP05(2013)098 [arXiv:1212.2643 [hep-th]].

[22] S. Kundu and J. F. Pedraza, "Aspects of Holographic Entanglement at Finite Temperature and Chemical Potential," JHEP **08** (2016), 177 doi:10.1007/JHEP08(2016)177 [arXiv:1602.07353 [hep-th]].

[23] Robert M. Wald, General relativity, Chicago Univ. Press, Chicago, IL, 1984.

[24] T. Faulkner, A. Lewkowycz and J. Maldacena, "Quantum corrections to holographic entanglement entropy," JHEP **11** (2013), 074 doi:10.1007/JHEP11(2013)074 [arXiv:1307.2892 [hep-th]].